Global and Planetary Change 175 (2019) 1–12

Contents lists available at ScienceDirect

Global and Planetary Change

journal homepage: www.elsevier.com/locate/gloplacha

The Holocene salinity history of Lake Lop Nur (Tarim Basin, NW China) inferred from ostracods, foraminifera, ooids and stable isotope data

Steffen Mischke[a,*], Chengjun Zhang[b], Chenglin Liu[c], Jiafu Zhang[d], Pencheng Jiao[c], Birgit Plessen[e]

[a] Faculty of Earth Sciences, University of Iceland, Reykjavík 101, Iceland
[b] School of Earth Sciences and Key Laboratory of Mineral Resources in Western China, Lanzhou University, Lanzhou 730000, China
[c] MLR Key Laboratory of Metallogeny and Mineral Assessment, Chinese Academy of Geological Sciences, Institute of Mineral Resources, Beijing 100037, China
[d] MOE Laboratory for Earth Surface Processes, Department of Geography, College of Urban and Environmental Sciences, Peking University, Beijing 100871, China
[e] Helmholtz Centre Potsdam, German Research Centre for Geosciences, Potsdam 14473, Germany

ARTICLE INFO

Keywords:
Arid Central Asia
Xinjiang
The Wandering Lake
Saline lakes
Microfossils
Palaeoecology

ABSTRACT

Terminal lakes without outlet respond directly to climate change and human impact, and provide important evidence for environmental conditions prior to times of instrumental monitoring. Lop Nur in northwestern China is a terminal lake which was still one of the world's largest lakes in historical times. Sediments from the excavated section YKD0301 in its presently dry basin were investigated to reconstruct the Holocene salinity history of the lake. Ostracod shells of *Cyprideis torosa* and *Eucypris mareotica*, tests of the foraminifer *Ammonia tepida*, and fruits of *Ruppia maritima* are abundant in the early Holocene part of the section. Two stratigraphic units in the middle Holocene part of the section contain ostracod shells typical of fresh to mesohaline waters such as *Limnocythere inopinata*, *Cypridopsis vidua*, *Ilyocypris* sp. and *Darwinula stevensoni*. Three units do not contain fossils or only few remains regarded as allochthonous. Ooids are abundant in the upper half of the section, and are here reported for the sediments of Lop Nur or sub-recent sediments from China for the first time. Ooids from YKD0301 are aragonitic and either subspherical around a detrital nucleus, or elongate and probably formed around fecal pellets of brine shrimps. The recorded fossils from Lop Nur indicate that lake waters were poly- to hyperhaline (20–100‰) at ca. 9.0 ka, oligo- to mesohaline (0.5–18‰) between ca. 8.7–7.5 ka and probably mesohaline (5–18‰) from 6.0–5.0 ka. In the intervening periods and after 5.0 ka, Lop Nur was a hyperhaline (> 100‰) lake. The period of freshest conditions of Lop Nur (ca. 8.7–7.5 ka) coincides with wettest Holocene conditions reconstructed from other lake records in the region although a uniform temporal pattern of wettest Holocene climate conditions in NW China and adjacent regions cannot be inferred.

1. Introduction

Lop Nur ('Nur' [Mongolian] for lake) is a large playa in the most arid region of Central Asia. The playa is located in the lowermost part of the endorheic Tarim Basin in China's northwesternmost province Xinjiang (Fig. 1). Lop Nur received a lot of attention as the '*Wandering Lake*' explored by the Swedish researcher Sven Hedin and his team in the early 20th century (Hedin, 1942). In addition, the discovery of the ruins of the Silk Road oasis Loulan in the northwestern vicinity of the dried lake by Hedin in 1900 initiated subsequent archaeological research in the region. Long rivers including the Tarim, the Konqi and Cherchen rivers fed Lop Nur before its final desiccation in the late 1930s or early 1940s (Li et al., 2008). Today, Lop Nur is a discharge playa with groundwater usually < 1 m beneath the surface (Ma et al., 2010).

The ancient lake was called 'Puchang Sea' during the Han Dynasty (206 BCE-220 CE; Ban, 1962). Historical documents from Han Dynasty times imply that the lake once covered an area of ca. 18,000–31,000 km^2, and was therefore one of the largest lakes on Earth (Yang et al., 2006). Mischke et al. (2017) suggested that Lop Nur underwent a similar crisis as today's Aral Sea during and after the Han Dynasty. Topographic surveys and analyses of excavated sediment sections and drilled cores were conducted in recent years to reveal the Pleistocene and Holocene history of Lop Nur and to better understand the significance of concentric lines seen in satellite images and called the 'Great Ear', and the formation of the salt crust in the basin's centre (Fig. 1B, Li et al., 2008; Dong et al., 2012). Long sediment cores from the Lop Nur region enabled the reconstruction of the general depositional history in the Quaternary, but the lake's more recent Holocene history remained poorly understood (Wang et al., 1999; Hao et al.,

* Corresponding author at: University of Iceland Faculty of Earth Sciences, Sturlugata 7101, Reykjavík, Iceland.
E-mail address: smi@hi.is (S. Mischke).

https://doi.org/10.1016/j.gloplacha.2019.01.017
Received 31 August 2018; Received in revised form 28 December 2018; Accepted 28 January 2019
Available online 30 January 2019
0921-8181/

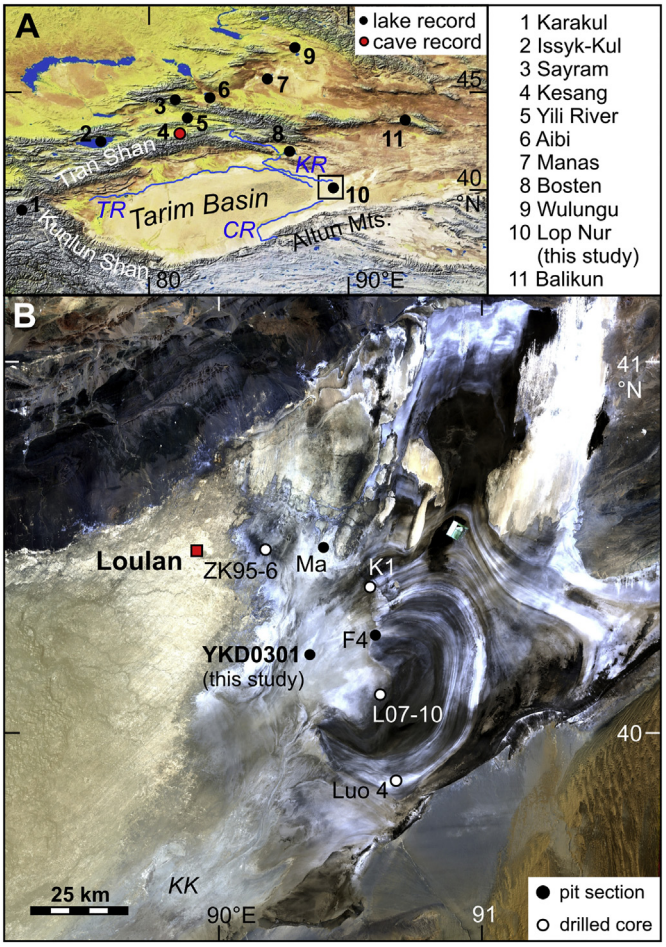

Fig. 1. A, Tarim Basin in NW China with location of Lop Nur (10) and other lake and cave records from the region. Main tributaries of Lop Nur are from north to south the Konqi (KR), Tarim (TR) and Cherchen (CR) rivers. B, region shown as rectangle in A. Lop Nur Basin and locations of the investigated YKD0301 and other sections and drilled cores, and the ruins of Loulan. *KK* indicates the region of Lake Kara Koshun which was fed by the Tarim River in 1877 (Prejevalsky, 1879).

2012). Excavated sections and drilled cores usually lack well-constrained chronologies due to the absence of suitable materials for radiocarbon dating in hyperarid environments. An exception is section YKD0301 where Zhang et al. (2012) used 22 samples for radiocarbon dating of the humin fraction and ten samples for optically stimulated luminescence (OSL) dating. Other sediment sequences in the Lop Nur region such as the section Ma were dated by only three or less radiocarbon samples (Fig. 1B; Ma et al., 2008). Liu et al. (2016) used sedimentological and geochemical data from the upper 4.65 m of section YKD0301 for a first assessment of the Holocene history of Lop Nur.

We here present new palaeontological and stable isotope data for the complete 5.7-m thick YKD0301 section to discuss the lake's history with special emphasis on the Holocene salinity changes.

1.1. Study area

The Tarim Basin is one of the largest endorheic basins on Earth with an area of > 530,000 km^2. It is surrounded by the Tian Shan ('Shan' [Chinese] for mountains), the Pamirs Plateau, the Kunlun Shan, the Altun Mountains and the Beishan which are mostly > 4000 m high above sea level (asl). The Tarim Basin is inclined from southwest (1300 m asl) to northeast (800 m asl) and its longest river, the Tarim River, flows west-east along the southern foothills of the Tian Shan. Kaidu River drains the eastern Tian Shan, enters Lake Bosten and flows as Konqi River to the Tarim Basin. The Cherchen River flows northeastward along the northern foreland of the Altun Mountains (Fig. 1).

Mountain regions in the catchment of Lop Nur are dominated by Palaeozoic rocks whilst the centre of the Tarim Basin is covered by the mobile sand dunes of the Taklamakan Desert. Wind-eroded remnants of Quaternary fluviolacustrine sediments called Yardangs are located in the northeastern vicinity of the playa.

The large distance to the oceans and shading of surrounding mountains causes hyperarid conditions in the Tarim Basin. Annual precipitation is 22.9 mm and potential evaporation is ca. 2700 mm at Ruoqiang 230 km to the southwest of Lop Nur. The Westerlies provide significantly higher precipitation in the surrounding mountain ranges of the Tarim Basin. Mean January, July and annual temperatures at Ruoqiang are −8.0, 27.4 and 11.6 °C, respectively (WorldClimate, www.worldclimate.com).

Vegetation is mostly constrained as gallery forests to ephemeral rivers (*Populus, Tamarix*) or consists of sparsely distributed desert vegetation (*Achnatherum*, *Stipa*, *Ajania*, *Artemisia*, *Ceratoides*, *Haloxylon*, *Ephedra*, *Tamarix*, *Suaeda* and *Kalidium*; Hou, 2001). Water from the middle reaches of the rivers which once entered Lop Nur is now intensively used for irrigation farming. The Lop Nur region itself is exploited for potash resources since the year 2004 by concentrating potassium-rich groundwater brines in artificially created evaporation ponds.

2. Materials and methods

2.1. The sampled section and its chronology

The YKD0301 section was excavated in the western part of the 'Great Ear' region in the year 2003. The section was continuously sampled without gap for grain-size and soluble salt analyses (Liu et al., 2016). The uppermost 0.28 m of the sequence represent salt-indurated sediments and a massive layer of rock salt on top which was not sampled for analysis of fossil remains. Radiocarbon and OSL dating of sediment samples revealed a Holocene age of the exposed section with a maximum age of 9.4 ka (ka - 1000 years) at the base 5.7 m beneath the playa surface (Zhang et al., 2012). The obtained radiocarbon ages were stratigraphically inconsistent beneath a depth of 1.12 m and were apparently all biased towards older ages as a result of the incorporation of 'dead' carbon (Zhang et al., 2012). Therefore, the available ten OSL data were used to establish an age-depth model and for first palaeoenvironmental inferences based on sedimentological and geochemical analyses (Liu et al., 2016; Mischke et al., 2017). The sedimentological characteristics and OSL age data suggest that sediments were accumulated at the section location continuously (Zhang et al., 2012; Liu et al., 2016).

2.2. Grain size analysis

In addition to grain-size data for the section above 4.65 m depth published by Liu et al. (2016), grain size of 33 samples from beneath 4.65 m depth was measured at 3-cm intervals with a Malvern Mastersizer 2000 laser diffraction particle size analyzer at the MOE Key Laboratory of Western China's Environmental Systems at Lanzhou University. Prior to analyses, sub-samples were treated with H_2O_2 to remove organic matter and soluble salts, with diluted 1 N HCl to remove carbonate and with Na-hexametaphosphate to disperse aggregates.

2.3. Analyses of total organic carbon (TOC) and carbonate content

TOC and carbonate content were measured at 3-cm intervals for 145 samples at Lanzhou University. TOC concentrations were measured using the anti-titration method with concentrated sulfuric acid (H_2SO_4)

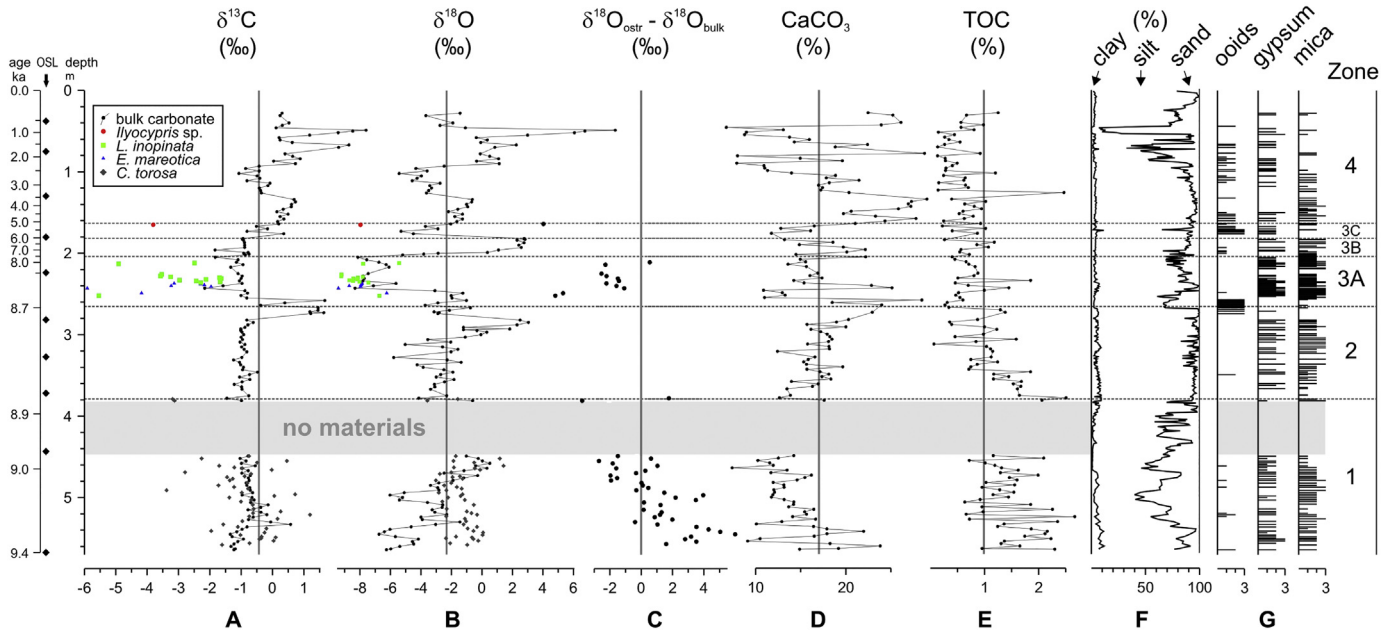

Fig. 2. Stable isotope data for bulk carbonate and ostracod shells (A-B), the difference between $\delta^{18}O_{bulk}$ and $\delta^{18}O_{ostr}$ (corrected for known vital effects) data for material from same stratigraphic levels (C), carbonate (D) and total organic carbon (TOC; E) concentrations, the grain size fractions clay, silt and sand (F), and the abundance of abiotic components in sieve residues (using a semi-quantitative scale: 0 – none, 1 – few, 2 – moderate, 3 – many; G). (For interpretation of the references to color in this figure legend, the reader is referred to the web version of this article.)

and potassium dichromate ($K_2Cr_2O_7$). The carbonate content was determined by treating bulk sediment samples with dilute 1 N HCl and measuring the generated CO_2 volume.

2.4. Analyses of fossil remains and abiotic components of sieve residues, and application of transfer function

Sub-samples for fossil-based analyses of 1 cm thickness were collected at intervals of ca. 2 cm from original sample material stored at the Institute of Mineral Resources, Chinese Academy of Geological Sciences in Beijing. Sample material was not available for the section from 3.82–4.47 m depth. A total of 231 sub-samples with a mean weight of 16 g were treated at the Institute of Geological Sciences of the Free University of Berlin, Germany. Sediments were soaked in 3% H_2O_2 solution for 48 h and washed through 100 and 250 µm sieves. Sieve residues were dried at 50 °C in an oven, and fossils picked under a low-power binocular microscope. All ostracod shells, charophyte remains and macrophyte fruits and seeds were collected from the sieve residues. Up to 1000 foraminifera tests were picked from each sample. After 1000 foraminifera tests were collected from a sample, the remaining sieve residue was spread on a picking tray and count data for five cells were extrapolated to the full area of 45 cells to estimate foraminifera abundances for nine samples containing > 1000 tests.

The abundances of ooids, gypsum crystals and mica grains in sieve residues > 100 µm were assessed semi-quantitatively using four classes: 0 – none, 1 – few, 2 – moderate, and 3 – many. The mineralogy of ooids was determined with a Rigaku MiniFlex XRD diffractometer at the Physical Geography lab of the Free University of Berlin, Germany. Powdered ooids from 1.71 and 2.58 m depth were scanned from 5 to 43°.

Ca. 50 ooids from a sample from 1.71 m depth were picked from the sieve residues and mounted in resin on glass slides to prepare thin sections. The sections were examined using a Leica DM750P microscope and images were made with a Leica EC3 camera. Surface textures and broken sections of ooids were further investigated using a Zeiss Supra 40 VP scanning electron microscope (SEM) at Freie Universität Berlin. In addition, ostracod shells and foraminifera tests were documented with the SEM.

An ostracod-based transfer function developed for the Tibetan Plateau was applied to roughly estimate specific conductivities (SCs) as proxy for past lake water salinity for ostracod species assemblage data of 25 samples containing at least 12 shells and including three or more taxa (Mischke et al., 2007). The transfer function was run in the software C2 (version 1.3) with the ostracod percentage abundances for the YKD0301 section as supplementary data.

2.5. Stable isotope analyses

Stable oxygen and carbon isotope analyses were carried out using a set of sub-samples of bulk sediments and a second set of selected well-preserved shells of adult ostracods. Stable isotope analysis of bulk material was carried out at the Lanzhou Institute of Geology, Chinese Academy of Sciences. Sub-samples were powdered and baked at 300 °C for 1 h in a vacuum system, and reacted with 100% H_3PO_4 at 90 °C. The produced CO_2 was trapped in a cold finger with liquid nitrogen and transferred into a Finnigan MAT 252 isotopic ratio mass spectrometer (IRMS).

Stable isotope analysis of ostracod shells was conducted at the German Research Centre for Geosciences in Potsdam. On average, 50 µg of shell material (11 shells of *Limnocythere inopinata*, six shells of *Eucypris mareotica*, two shells of *Cyprideis torosa*) were reacted with 103% H_3PO_4 at 70 °C in an automated carbonate preparation device (KIEL IV) coupled to a Finnigan MAT 253 IRMS. Isotopic ratios are given in delta notation relative to VPDB (Vienna Pee Dee Belemnite) calibrated with NBS-19 ($\delta^{18}O = -2.20‰$). The analytical precision of the $\delta^{18}O$ and $\delta^{13}C$ values is better than ± 0.06‰ for the ostracod shell ($\delta^{18}O_{ostr}$) and ± 0.3‰ for the bulk carbonate ($\delta^{18}O_{bulk}$) samples (1σ).

The $\delta^{18}O_{bulk}$ values were compared with the $\delta^{18}O_{ostr}$ values to assess potential effects of lake-level changes and thermal or chemical stratification of the water column. Ostracod shells commonly have higher $\delta^{18}O$ values than carbonate formed in isotopic equilibrium due to vital effects (von Grafenstein et al., 1999). The $\delta^{18}O_{ostr}$ values were therefore corrected by −0.80‰ for *Cyprideis torosa*, by −0.78‰ for *Limnocythere inopinata*, and by 0.32‰ for *Ilyocypris* (von Grafenstein et al., 1999;

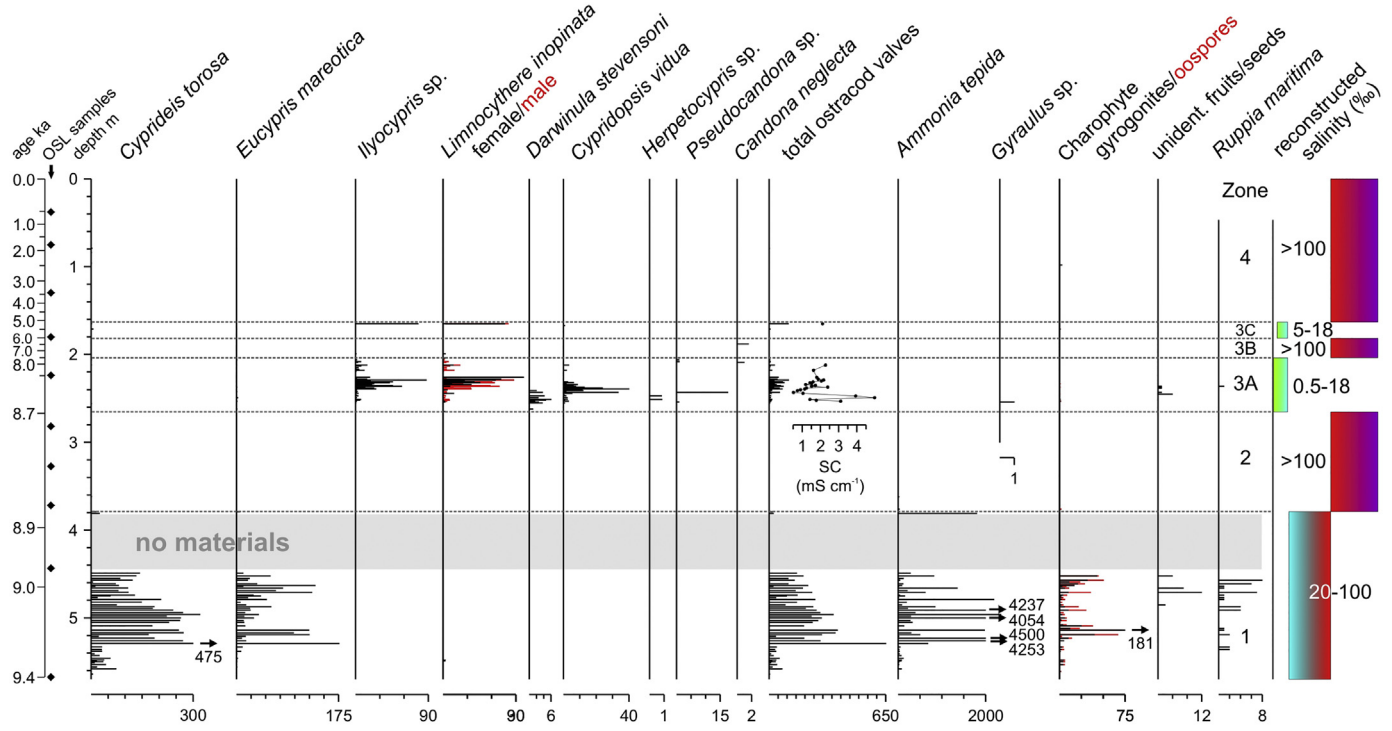

Fig. 3. Absolute abundances of ostracod shells, tests of the foraminifer *Ammonia tepida*, charophyte remains, unidentified plant diaspores and fruits of *Ruppia maritima* in section YKD0301. Reconstruction of specific conductivity (SC) in Zone 3 is based on transfer function of Mischke et al. (2007). Schematic salinity inferences for the different zones at the right.

Keatings et al., 2007; Mischke et al., 2008). The $\delta^{18}O_{ostr}$ values for *Eucypris mareotica* were not corrected due to the formation of shells almost in isotopic equilibrium with host water demonstrated by Li and Liu (2010).

3. Results

Grain size analysis of sediments beneath 4.65 m depth revealed that sediments mostly consist of silt (38–89%) or sand (3–60%). Clay-sized particles occur in a range from 2 to 12% (Fig. 2F). TOC concentrations are between 0.1 and 2.7% with a mean and standard error of 1.0 ± 0.1%. Carbonate content is in a range from 6.7–29.0% with a mean of 16.7 ± 0.4% (Fig. 2D).

A total of 9055 ostracod shells of nine species were found in the sediments of the YKD0301 section (Fig. 3). Most abundant are shells of *Cyprideis torosa*, followed by shells of *Eucypris mareotica* and those of female and male specimens of *Limnocythere inopinata* (Figs. 3 and 4). Shells or *C. torosa* and *E. mareotica* mostly occur in sediments beneath 3.79 m depth, and shells of *L. inopinata* and other taxa such as *Cypridopsis vidua* and *Ilyocypris* sp. are abundant in sediments between 2.55 and 2.12 m. The ostracod-based SC reconstruction yielded values in a range from 0.5–5.0 mS cm^{-1} or of 1.8 mS cm^{-1} on average.

Tests of the foraminifer *Ammonia tepida* are abundant in sediments beneath 3.79 m depth. Charophyte gyrogonites and oospores were frequently recorded in sediments below 4.50 m depth. A single gastropod shell of *Gyraulus* sp. was recorded at 2.54 m. Fruits of *Ruppia maritima* mostly occur beneath 4.56 m depth and additional undetermined fruits or seeds were recorded at 4.85–4.52 m and 2.45–2.36 m depth (Fig. 3). Gypsum crystals and mica grains were recorded in almost all parts of the section and ooids mostly in its upper half. Ooids are either more or less spherical with individual nuclei of detrital material such as quartz or rod-shaped around fine grained aggregated sediments (Fig. 5). XRD analysis showed that aragonitic layers form the carbonate cortex of ooids. Aragonite crystals are either equidimensional-microgranular or radially arranged.

The $\delta^{18}O_{bulk}$ values range from −8.3 to 8.7‰ (mean: −2.3 ± 0.2‰) and the $\delta^{18}O_{ostr}$ values from −9.4 to 1.4‰ (mean: −2.9 ± 0.4‰; Figs. 2 and 6). $\delta^{13}C$ values of bulk carbonate ($\delta^{13}C_{bulk}$) are in a range from −2.2 to 3.0‰ (mean: −0.4 ± 0.1‰). The $\delta^{13}C$ values for ostracod shells ($\delta^{13}C_{ostr}$) are between −5.9 and 1.2‰ (mean: −1.6 ± 0.2‰). Differences between $\delta^{18}O_{ostr}$ and $\delta^{18}O_{bulk}$ values from similar stratigraphic levels in the YKD0301 section range from −6.2 to 6.0‰ (mean: 0.1 ± 0.4‰; Fig. 2C).

4. Discussion

4.1. Lake conditions inferred from the YKD0301 data

Four stratigraphic zones were established for the YKD0301 section based on a combination of recorded changes of the ostracod and foraminifera assemblage and prominent changes of the $\delta^{18}O_{bulk}$ data (Figs. 2 and 3).

Zone 1 (5.70–3.79 m; ~9 ka).

Sediments of Zone 1 (Z1) are dominated by silt near the lower and upper zone boundaries and by sand and silt in its middle section. Shells of the ostracods *C. torosa* and *E. mareotica* are abundant, and those of both species, of the thick-shelled *C. torosa* and also the thin-shelled *E. mareotica* are well preserved and not fragmented or significantly altered by corrosion or recrystallization (Fig. 4). Shells of juvenile and adult specimens are similarly recorded, and shell formation at or near the section location without significant post-mortem transportation is inferred. In addition to abundant ostracod shells, tests of the foraminifer *A. tepida*, charophyte gyrogonites and oospores, and fruits of *R. maritima* and other plants were recorded.

The $\delta^{18}O_{bulk}$ values are mostly in a low to moderate range from −6 to −2‰ in the lower half of the zone and − 2 to 1‰ closer to the top.

The $\delta^{18}O_{ostr}$ values for *C. torosa* shells scatter around −1.3‰ and are mostly higher than $\delta^{18}O_{bulk}$ values from the same stratigraphic levels (Fig. 2B-C). Carbonate contents fluctuate rapidly at the base of Z1 between ca. 10–22% and decrease to ca. 12% in the upper part of the

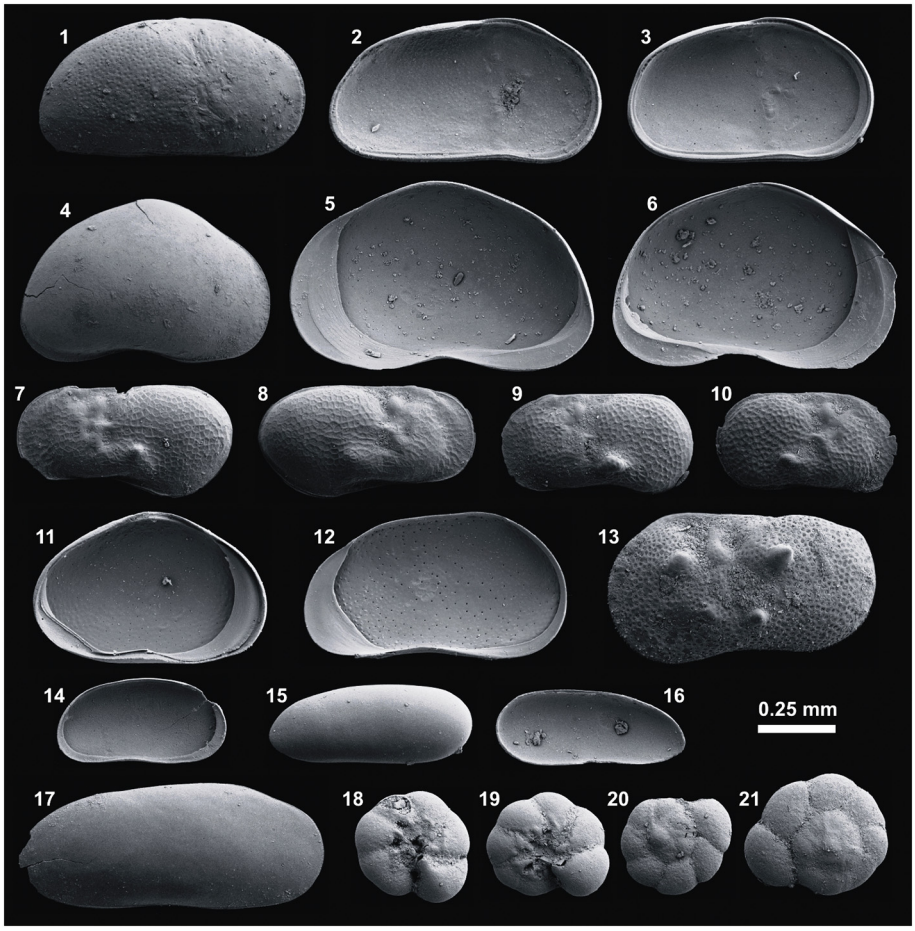

Fig. 4. Ostracod shells and foraminifer tests (18–21) from section YKD0301 in Lop Nur. *Cyprideis torosa*: 1 ♂ right shell (RS) external view (ev), 2 ♂ left shell (LS) internal view (iv), 3 ♀ LS iv; *Eucypris mareotica*: 4 RS ev, 5 RS iv, 6 LS iv; *Limnocythere inopinata*: 7 ♂ LS ev, 8 ♂ RS ev, 9 ♀ LS ev, 10 ♀ RS ev; 11 *Cypridopsis vidua* LS iv; 12 *Pseudocandona* sp. RV iv; 13 *Ilyocypris* sp. LS ev; 14 *Candona* cf. *neglecta* (juvenile) LS iv; *Darwinula stevensoni*: 15 LS ev, 16 LS iv; 17 *Herpetocypris* sp. (juvenile) RS ev; *Ammonia tepida*: 18 and 19 umbilical views, 20 and 21 spiral views. All specimens housed at Institute of Geological Sciences, Free University of Berlin (Germany).

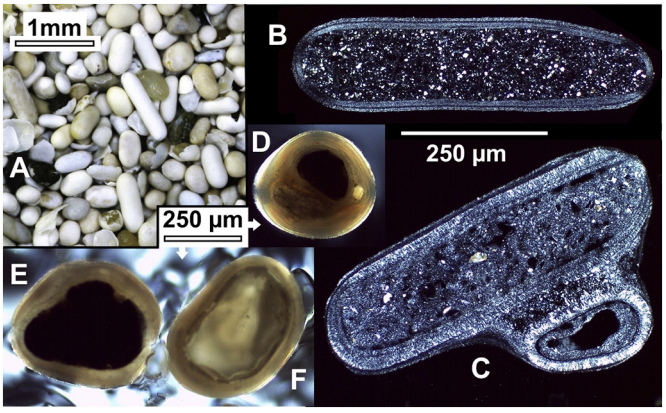

Fig. 5. Ooids from Lop Nur. A, ooids and uncoated detrital grains in the > 250 µm sieve residue fraction. B, ooid formed around fecal pellet. C, two cemented ooids formed around fecal pellets and with aragonite layers predominantly composed of radially arranged crystals. D, ooid formed around three detrital grains. E-F, ooids formed around individual detrital grains.

zone, and TOC concentrations are relatively high (1–2%) in Z1. Sample materials were not available for most analyses between 4.47 and 3.82 m depth but two samples above this gap contained abundant shells of *C. torosa* and *E. mareotica*, and many tests of *A. tepida*. Thus, these two samples were included in Z1.

The abundant shells of *C. torosa* and *E. mareotica*, the tests of *A. tepida*, the charophyte remains, and the fruits of *R. maritima* and other plants in the mostly silty and partly sandy sediments of Z1 indicate that Lop Nur was a stable brackish to possibly hyperhaline lake in the early Holocene. The recorded fossils originate from organisms with relatively well-known ecological requirements and generally wide salinity tolerance ranges (Table 1). Charophytes are mostly known to occupy fresh and brackish waters but species such as *Lamprothamnium papulosum* tolerate permanently hyperhaline conditions of two or even three times sea-water salinity (Davis and Lipkin, 1986). The shared optimum salinity range of the identified ostracod, foraminifer and aquatic plant species lies within 13.0–16.5‰ (Table 1). However, the absence of shells of ostracod taxa such as *Limnocythere inopinata, Sarscypridopsis aculeata* or *Heterocypris salina,* which commonly tolerate upper mesohaline conditions, suggests that salinity levels were mostly if not generally higher (Mischke et al., 2007, 2008; Mischke and Zhang, 2011). *Ammonia tepida* and *C. torosa* have probably the lowest maximum salinity tolerance in a range from 90 to 100‰ of the four taxa in Z1 (Walton and Sloan, 1990; Drapun et al., 2017). Thus, poly- to hyperhaline conditions, probably in a range from ca. 20–100‰ are inferred for Lop Nur during Z1. Although gypsum may have partly been formed diagenetically, the abundant lenticular gypsum in sediments of Z1 probably indicates that Lop Nur waters were saturated with respect to gypsum and had salinities of > 150‰ at least from time to time (Warren, 2006). Evaporation experiments of brines from the Great Ear region and the middle reaches of the Tarim River suggest that gypsum saturation is reached at ca. 188‰ in modern waters (Sun et al., 2016).

The first significant maximum in the sand fraction at 5.24 m and the largest and bifurcated maximum in Z1 at 5.03 and 4.97 m depth correspond to a less pronounced $\delta^{18}O_{bulk}$ minimum and a more significant and also bifurcated $\delta^{18}O_{bulk}$ minimum, respectively (Fig. 2B,F). Relatively coarse-grained sediments apparently do not reflect lowered lake levels and more evaporated waters but they probably indicate strong inflows to the lake and the delivery of detrital sediments. The sand-

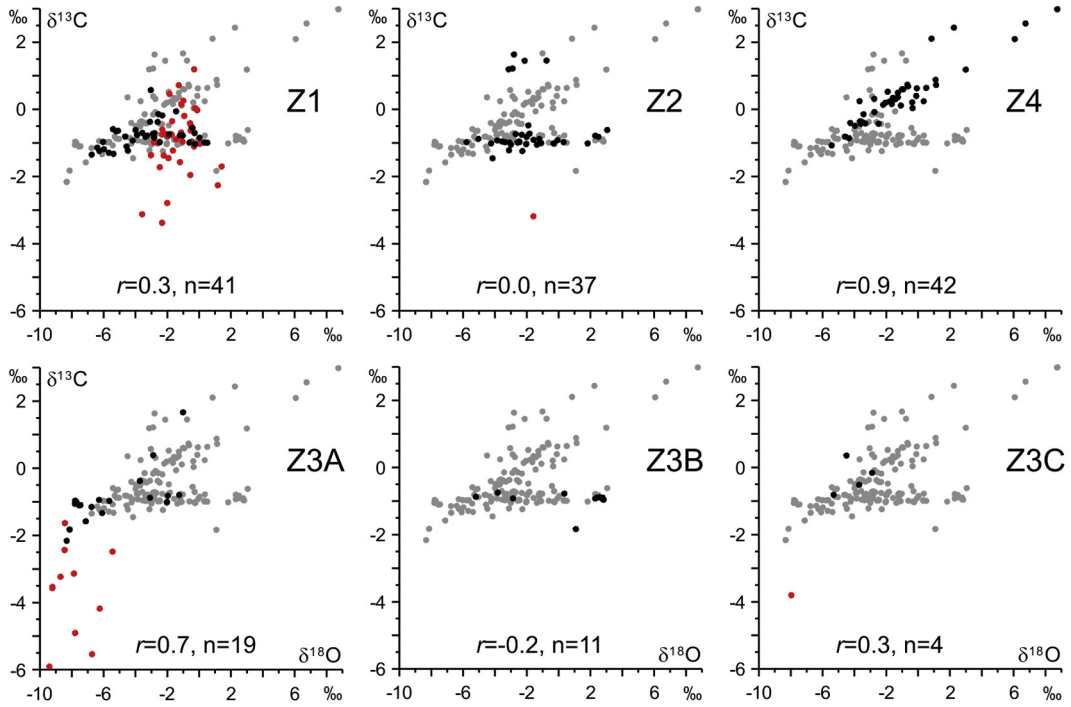

Fig. 6. $\delta^{18}O$ and $\delta^{13}C$ crossplots for the individual zones and subzones of the YKD0301 section. Grey dots indicate all $\delta^{18}O_{bulk}$ and $\delta^{13}C_{bulk}$ data, black dots indicate the data for the specific zone and red dots the $\delta^{18}O_{ostr}$ and $\delta^{13}C_{ostr}$ values for the zone which were not corrected for vital effects. (For interpretation of the references to colour in this figure legend, the reader is referred to the web version of this article.)

Table 1
Salinity tolerance and optimum information (in ‰) for taxa recorded in sediments of the YKD0301 section.

Taxon	Minimum tolerance	Optimum minimum	Optimum maximum	Maximum tolerance	References
Cyprideis torosa	0.4	2	16.5	100	Meisch (2000); Drapun et al. (2017)
Eucypris mareotica	2.8	2.8	106	325	Schornikov (1964); Williams (1991)
Ammonia tepida	1	13	40	> 90	Walton and Sloan (1990); Almogi-Labin et al. (1992)
Artemia	4	35	110	370	Shadrin and Anufriieva (2012); Vanhaecke et al. (1984)
Ruppia maritima	0.6	5	22	390	Kantrud, 1991
Charophyta	0.1	–	–	125	Davis and Lipkin (1986)

fraction maxima also correspond to maxima in abundances of *C. torosa* shells and *A. tepida* tests suggesting the improvement of habitat conditions during these periods of strong inflows (Fig. 3). The increasing abundances of *C. torosa* and *A. tepida* during times of strong freshwater inflows support the inference of mostly hyperhaline conditions in Lop Nur with salinities mostly above the species-specific salinity optimum ranges of 2–16‰ and 13–40‰, respectively (Table 1). During times of strong freshwater inflow in Z1, salinities were probably within or relatively close to these ranges. A relatively high water depth during the lower half of Z1 is also indicated by the higher $\delta^{18}O_{ostr}$ values in comparison to $\delta^{18}O_{bulk}$ values (Fig. 2B-C). Significantly higher $\delta^{18}O_{ostr}$ values probably result from lower bottom-water temperatures and/or higher bottom-water salinities in comparison to surface waters and thus, stratification of the water column.

Relatively dilute surface waters above a saline bottom-water layer are also suggested by the absolute $\delta^{18}O_{bulk}$ values in comparison to those reported for the open-basin Lake Bosten. Lake Bosten is fed by the Kaidu River and its outflow feeds the Konqi River as one of the major tributaries of Lop Nur (Fig. 1A). The $\delta^{18}O_{bulk}$ values for the last 8.5 ka of Lake Bosten fluctuate in a range from −7 to 0‰ which is more or less similar to $\delta^{18}O_{bulk}$ fluctuations in Z1 (Zhang et al., 2010). Thus, evaporation effects on host waters of carbonate formation were apparently not significant in Lop Nur, and we infer that authigenic carbonate was predominantly formed in inflow regions and subsequently distributed in the Lop Nur Basin by wind-driven currents.

In contrast to coinciding maxima of the sand fraction and $\delta^{18}O_{bulk}$ minima at 5.24, 5.03 and 4.97 m depth, the bifurcated sand-fraction maximum at 4.65 and 4.60 m depth corresponds to a similarly bifurcated maximum of the $\delta^{18}O_{bulk}$ values. Here, a more efficient mobilization of detrital particles resulted from diminished inflows to Lop Nur which led to lowered lake levels and evaporative concentration of lake waters. This inference is supported by a peak of *E. mareotica* abundances which probably has a high salinity optimum maximum of ca. 106‰ (Schornikov, 1964). Slightly higher numbers of *R. maritima* fruits are in contradiction to the inference of high salinities at 4.65–4.60 m depth in Z1, but probably result from the drift of fruits from relatively nearby regions of inflows or of relatively dilute spring-discharge waters. Increasing numbers of charophyte gyrogonites and oospores probably also originate from more dilute waters which existed possibly not far from the section location.

The lower and upper sand-fraction maxima are accompanied by the presence of ooids in sediments of Z1 (Figs. 2 and 5). Ooid formation requires $CaCO_3$ supersaturation, the presence of nuclei, agitation of the grains and a setting which retains the grains in the system (Bathurst, 1971). Ooids are rarely reported from recent or sub-recent non-marine environments and most records originate from the hyperhaline Great Salt Lake in Utah (salinity 190–275‰) or Lake Urmia in Iran (salinity 202‰; Halley, 1977; Kelts and Sharabi, 1986). Although ooids may form in freshwater settings, the similarity of radially oriented aragonitic ooids from Lop Nur with those described from the Great Salt Lake and

the lack of irregular micritic particles having cauliflower shapes such as those from Lake Geneva suggests formation in a hyperhaline environment (Fig. 5; Halley, 1977; Wilkinson et al., 1980; Davaud and Girardclos, 2001). Moreover, the partly rod-shaped ooids with up to 1 mm length from Lop Nur resemble the elongate ooids from Lake Urmia and the Great Salt Lake which formed around fecal pellets of the brine shrimp *Artemia* (Fig. 5; Sandberg, 1975; Kelts and Shahrabi, 1986). The very flat basin topography of today's salt-crust covered playa with a maximum relief of 5.2 m in the 'Great Ear' region probably provided an excellent setting for ooid formation where particles were agitated in shallow waters for a sufficiently long period of time (Li et al., 2008). *Artemia* has a salinity optimum between ca. 35–110‰, and the assumed formation of elongate ooids around fecal pellets further supports the inference of a hyperhaline lake in the early Holocene (Vanhaeke et al., 1984). Brine shrimps occur in hyperhaline lakes in Xinjiang today (Vanhaecke et al., 1987).

The presence of subspherical and elongate ooids in the Holocene sediments of Lop Nur indicates that detrital grains and fecal pellets were present as nuclei for ooid formation, that waters were supersaturated with respect to carbonate, and that grains were agitated in shallow water of a few meters depth and held sufficiently long in the system. However, the absence of ooids from some parts of Z1 does not indicate either desiccation or larger water depths due to the possibility that other controlling factors than depth were possibly inhibiting ooid formation and accumulation at the section location (lack of nuclei, adverse micro-relief or local currents).

Based on grain-size, soluble salt and pollen data, Liu et al. (2016) inferred shallow brackish lake conditions with diminishing floods in a steppe environment for sediments of Z1 above 4.65 m depth. Our record of ooids in the sediments of Z1 is consistent with the inference of shallow lake conditions by Liu et al. (2016). However, our fossil-based inference of a salinity in a range from 20 to 100‰ represents a more precise estimate of Lop Nur's salinity at 9 ka.

The OSL age data of the YKD0301 section imply that the relatively thick sediments of Z1 were accumulated within a short period of time of a few hundred years (Zhang et al., 2012). Estimated sediment accumulation rates (SARs) are ca. 4 mm a^{-1}. A massive sediment delivery to the lake at ca. 9 ka might be explained by three scenarios: (1) the delivery of detrital sediments to Lop Nur may have resulted from the melting of glaciers in the high mountain ranges surrounding the Tarim Basin after late glacial advances centered on the Younger Dryas period. Regional glacier advances were reviewed and termed 'semi-arid western Himalayan-Tibetan stage' (SWHTS) 2A by Dortch et al. (2013). Alternatively or in addition, (2) large volumes of loess sediments were possibly washed to the tributaries of Lop Nur as a result of an increase in precipitation implied by a regional averaged moisture index for Xinjiang at ca. 9.6 ka by Wang et al. (2013; Jiang et al., 2013). Thick loess deposits are widespread in the piedmont regions and intramontane basins of Central Asia's mountain ranges, and exposed erosive remnants of thick alluvial loess deposits at few locations with exceptional preservation conditions in the eastern Tian Shan indicate that loess deposits covered significantly more extensive areas sometime in the Quaternary (Hofmann et al., 2002; Mischke et al., 2004; Li et al., 2016). Weakly consolidated sediment covers overlying basement rocks similar to those described by Hofmann et al. (2002) and Mischke et al. (2004) were possibly wide-spread in relatively dry mountain areas of Xinjiang and were possibly mostly eroded during the precipitation increase of the early Holocene. Furthermore, (3) high SARs possibly reflect low vegetation cover in the catchment of Lop Nur due to dry climate conditions which led to high sediment loads of tributaries and high influx of aeolian sediments (Liu et al., 2016). However, more research is required to better understand the early Holocene sediment dynamics in the region.

Zone 2 (3.79–2.66 m; ~8.8 ka).

Sediments in Z2 are dominated by silt (90%). The clay and sand fractions represent mostly portions of ca. 5%, each. Apart from a few ostracod shells and *A. tepida* tests in the lowermost samples, foraminifer tests were only occasionally detected with low numbers (≤5) in Z2. The $\delta^{18}O_{bulk}$ values are mostly in a range from −4 to −2‰ in the lower half of Z2 and mostly between −1 and 3‰ in the upper part. The $\delta^{13}C_{bulk}$ values are relatively constant apart from a few high values in the upper part of Z2. TOC values are relatively high near the base and moderate to low afterwards. The almost complete lack of organism remains probably results from salinities well above the optimum ranges of the taxa recorded in Z1. Therefore, salinities > 110‰ are inferred for Z2. Gypsum is even more abundant than in Z1 indicating salinities > 150‰ at least from time to time. TOC concentrations of 2% and less are evidence against the establishment of anoxic conditions at the lake floor as possible reason to explain the almost complete absence of fossils in Z2. Occasionally recorded *A. tepida* tests were probably reworked. High salinity and resulting low productivity in the lake is possibly also indicated by relatively low and stable $\delta^{13}C_{bulk}$ values in the lower and middle part of Z2 (Figs. 2 and 6). Apart from a few samples, $\delta^{13}C_{bulk}$ values vary in a narrow range and are not correlated to $\delta^{18}O_{bulk}$ values possibly reflecting high salinities and low productivity in the lake, and high alkalinity of lake waters and negligible CO_2 degassing (Fig. 6; Horton et al., 2016). In contrast, the occurrence of many ooids in the uppermost samples of Z2 is accompanied by a sharp drop of the $\delta^{18}O_{bulk}$ and an increase of the $\delta^{13}C_{bulk}$ values. Dilution of lake waters and an increase in productivity probably resulted from a strong freshwater inflow to Lop Nur in the uppermost part of Z2. Ooid formation was possibly triggered by the delivery of detrital materials to the lake which became available as nuclei. It remains unclear whether algae, bacteria or fungi contributed to ooid formation and benefited from more favourable conditions during times of lowered salinities in Lop Nur (Simone, 1981). The $\delta^{18}O_{bulk}$ values of mostly −4 to 0‰ are comparable to $\delta^{18}O_{bulk}$ fluctuations in the Holocene record from Lake Bosten (Zhang et al., 2010). Strong evaporation effects expected for carbonate formed in a closed-basin lake environment are not evident although the lack of abundant microfossils and the presence of gypsum in the sediments of Z2 indicate saline conditions. Thus, it is assumed that most carbonate formed near the inflows and was subsequently distributed over the lake basin.

Drier climate conditions and higher aeolian influx in Lop Nur were inferred from high *Ephedra* and low *Artemisia* pollen counts, high soluble salt contents and a lower sand portion in Z2 by Liu et al. (2016).

Similar to sediments of Z1, OSL age data imply high SARs of ca. 6 mm a^{-1} in Z2 (Zhang et al., 2012). Rapid sediment accumulation in Lop Nur and inferred higher salinities and decreasing inflows to the lake are possibly explained by decreasing glaciers and diminishing meltwater resources in the mountain ranges around the Tarim Basin and continuously high sediment loads of Lop Nur's tributaries (Dortch et al., 2013; Ran et al., 2015). In addition, aeolian influx to Lop Nur was probably efficient due to dry climate conditions and low vegetation cover in the region (Liu et al., 2016).

Zone 3 (2.66–1.65 m; ~8.7–5.0 ka).

Sediments of Z3 partly contain shells of ostracods typically found in fresh to oligo- or slightly mesohaline waters, and remains of plants and charophytes. The zone is subdivided in sub-zones Z3A, Z3B and Z3C.

Zone 3A (2.66–2.04 m; ~8.7–7.5 ka).

Z3A is characterized by silt-dominated sediments with relatively high portions of sand near the lower and upper sub-zone boundaries. TOC concentrations are generally low with slightly increased values in the middle of Z3A. Ooids occur in the lower part of Z3A. Abundances of ostracod shells are increasing from the base of Z3A towards the middle part, and decreasing near the top again. The dominating ostracod species *L. inopinata*, *C. vidua* and *Ilyocypris* sp. are widespread in Eurasia and adapted to a wide range of ecological conditions (Meisch, 2000). Together with less abundant shells of *D. stevensoni* and *Pseudocandona* sp., and few shells of *E. mareotica*, *C. torosa*, *Herpetocypris* sp. and *C. neglecta*, an oligo- to mesohaline lake with aquatic macrophytes and a depth not exceeding a few metres is inferred.

The presence of gypsum in sediments of Z3A either results from short-lived significant salinity increases or the re-deposition of gypsum grains which were formed earlier in Lop Nur. The latter is supported by lowest $\delta^{18}O_{bulk}$ values mainly in a range between −8 and − 6‰ which are similar to those of the Lake Bosten record between 8.5 and 7.5 ka (Zhang et al., 2010). The low $\delta^{18}O_{bulk}$ values indicate a significant dilution of lake waters due to strong inflows of freshwater. The ostracod shells do not show signs of post-mortem transportation, but generally lower $\delta^{18}O_{ostr}$ values in comparison to $\delta^{18}O_{bulk}$ values for individually sampled stratigraphic levels possibly indicate shell formation in regions closer to runoff inflows or discharging springs (Fig. 2B-C). Significantly lower $\delta^{13}C_{ostr}$ values in comparison to $\delta^{13}C_{bulk}$ values possibly support the inference that ostracod shells were formed in more dilute waters where $\delta^{13}C$ of dissolved inorganic carbon (DIC) was lower due to a higher productivity in fresher waters and remineralization of ^{12}C-enriched carbon from decaying organic matter and due to less efficient exchange of DIC with atmospheric carbon dioxide (Horton et al., 2016). Alternatively, ostracod shells may have predominantly been formed during seasons or years of relatively low salinities in Lop Nur whereas the $\delta^{18}O_{bulk}$ and $\delta^{13}C_{bulk}$ data possibly represent more saline seasons or years.

The application of the ostracod-based transfer function of Mischke et al. (2007) revealed SC values of ca. 1.8 mS cm^{-1} equivalent to salinities of ca. 1.2‰ (Hem, 1982). The species assemblage-derived SC changes closely follow the $\delta^{18}O_{bulk}$ data suggesting that both ostracod species and stable isotope data of bulk carbonate reliably reflect water chemistry changes in Lop Nur (Fig. SOM 1). Relatively similar assemblages but slightly lower numbers of taxa in Z3A in comparison to the modern ostracod fauna of Lake Bosten (SC: 0.2 mS cm^{-1}) and Lake Wulungu (= Ulungur; SC: 3.9 mS cm^{-1}) indicate that reconstructed SC values are probably slightly underestimated (Mischke and Schudack, 2001; Mischke and Zhang, 2011; Dai et al., 2014).

The ostracod fauna of Z3A especially resembles the modern fauna of Lake Wulungu, and a relatively similar water composition dominated by Na^+, Cl^- and SO_4^{2-} is inferred for Lop Nur. Present-day groundwater and spring brines in the Lop Nur region are dominated by Na^+ and Cl^-. They are poor in Ca^{2+} and $HCO_3^- + CO_3^{2-}$, but contain a considerable amount of Mg^{2+} and SO_4^{2-} (Ma et al., 2010). Although the ion composition of water was apparently not very different for Lop Nur waters during Z3A in comparison to today's brines in the region, the salinity was significantly lower in the lake. Lop Nur experienced a significant freshwater pulse during the accumulation of the Z3A sediments.

Correspondingly, wetter climate conditions were previously inferred from the section due to lower soluble salt contents, sediments of predominantly fluvial instead of aeolian origin, and higher Gramineae and lower *Ephedra* and *Pinus* counts (Liu et al., 2016).

In contrast to the inferred higher freshwater inflow in Lop Nur, the OSL age data for the YKD0301 section imply significantly reduced SARs of ca. 0.5 mm a^{-1} in Z3A (Zhang et al., 2012). Wetter climate conditions possibly led to denser vegetation cover in the region and a decrease in sediment mobilization by sheet floods and wind (Liu et al., 2016). In addition, we speculate that easily erodible sediments which were mostly accumulated as dust after the last interglacial in Marine Isotope Stage (MIS) 4 until the early-mid MIS 3 and during MIS 2 were not as widely distributed in the catchment of the lake after the early Holocene precipitation increase (Li et al., 2016).

Zone 3B (2.04–1.82 m; ~7.5–6.0 ka).

Sediments of Z3B are dominated by silt similar to those of Z3A. Carbonate contents are relatively high and TOC concentrations low (Fig. 2D-E). Only six ostracod shells were recorded in Z3B which were probably transported to the section location. Ooids occur in the middle of the zone. The $\delta^{18}O_{bulk}$ values show a dramatic increase at the base of Z3B and high values between 1 and 3‰ afterwards. $\delta^{18}O_{bulk}$ values from the same period of time of the Lake Bosten record are significantly lower with values mostly in a range from −6 to −2‰ (Zhang et al., 2010) indicating strong evaporation effects on the waters of Lop Nur in comparison to lake waters upstream of the Konqi River.

The almost complete absence of fossils, the high $\delta^{18}O_{bulk}$ values and almost stable $\delta^{13}C_{bulk}$ values resemble sediments of Z2, and hyperhaline conditions well above the optimum ranges of the taxa recorded in Z1 and Z3A are assumed (Figs. 2, 3 and 6). Thus, salinities were probably > 110‰ in Lop Nur and generally lower inflows in Lop Nur are inferred. Increasing soluble salt contents, and the decreasing mean grain size and inferred higher portion of aeolian sediments support the suggestion of more saline and generally drier conditions for Z3B although Liu et al. (2016) did not discuss more arid conditions after the accumulation of sediments of Z3A.

SARs in Z3B decreased to ca. 0.1 mm a^{-1} which is consistent with the inferred reduction of inflows and salinity increase in the lake.

Zone 3C (1.82–1.65 m; ~6.0–5.0 ka).

Sediments of Z3C resemble those of Z3A by their similar dominance of the silt fraction, low TOC and carbonate contents and relatively low $\delta^{18}O_{bulk}$ values (Fig. 2B,D-F). Shells of *L. inopinata* and *Ilyocypris* sp. occur only in the uppermost part of Z3C, and a few more shells of *C. torosa*, *E. mareotica* and *C. vidua* were recorded in the middle part of Z3C (Fig. 3). Similar to the uppermost part of Z2, ooids are abundant in Z3C and their presence is accompanied by increased $\delta^{13}C_{bulk}$ and lower $\delta^{18}O_{bulk}$ values. The ostracod shells and the $\delta^{13}C_{bulk}$ increase indicate a lower salinity and increased productivity in Lop Nur. However, the fossils in Z3C do not reach the abundances and diversity seen in Z3A, and strongly alkaline and mesohaline conditions are inferred from the predominance of shells of *L. inopinata* (Meisch, 2000). However, the $\delta^{18}O_{bulk}$ values are ca. -4‰ in Z3C and comparable to contemporary $\delta^{18}O_{bulk}$ values of the record from Lake Bosten between −6 and − 3‰ (Zhang et al., 2010). Thus, relatively insignificant evaporation effects on waters of Lop Nur are inferred. The $\delta^{18}O_{ostr}$ value for shells of *Ilyocypris* sp. from the uppermost part of Z3C is significantly lower than the value for bulk material from the same stratigraphic level and post-mortem transport of shells from more dilute waters in inflow or spring-discharge regions is assumed. In comparison to Z3A, gypsum is less abundant in Z3C and probably results from reworked material. Higher pollen concentrations and *Artemisia* counts, and lower *Ephedra* pollen abundances are consistent with inferred lower salinities and generally wetter conditions during the accumulation of sediments of Z3C (Liu et al., 2016). In contrast, relatively high soluble salt contents cannot be explained by a regional moisture increase but possibly result from postdepositional salt precipitation from pore fluids.

The OSL data imply only slightly increased SARs (0.2 mm a^{-1}) in Z3C. An increased freshwater inflow to Lop Nur apparently did not trigger significantly higher SARs at the section location possibly due to 1) denser vegetation cover in the catchment and diminished mobilization of sediments by surface runoff and wind, 2) larger distances to inflow areas during times of higher lake levels, and 3) sediment trapping in dense reed belts similar to the modern inflow of Kaidu River in Lake Bosten and described for the Lake Kara Koshun in 1877 by Prejevalsky (1879) when the Tarim River bypassed the dry Lop Nur Basin and fed a lake in its southwestern vicinity.

Zone 4 (1.65–0.28 m; ~5.0–0 ka).

Sediments are dominated by silt in the lower and upper part of Z4. In contrast, the sand fraction increases in the middle section of Z4 and partly reaches higher values than in Z1–3 (Fig. 2F). Only seven ostracod shells, five foraminifera tests and a single charophyte gyrogonite were found in five samples from Z4. All other 48 samples did not contain fossils, and the low number of detected organism remains indicates their allochthonous origin. Ooids are relatively abundant in Z4 but absent from the uppermost sediments. Gypsum generally occurs in Z4 but was not recorded between 1.5 and 1.2 m depth. Within this section, carbonate contents are high and salinities did apparently not reach gypsum saturation in Lop Nur. Given that modern brine compositions are not significantly different from Holocene brines, salinities were probably below ca. 188‰ during the gypsum-lacking sediments in Z4

(Sun et al., 2016). However, the lack of organism remains suggests that salinities were not lower than ca. 100‰ (Fig. 3).

The $\delta^{18}O_{bulk}$ values fluctuate mostly between −4 and 3‰ in Z4. They are similar or only slightly higher than the $\delta^{18}O_{bulk}$ values from the last 5 ka of the Lake Bosten record (−6 to 0‰; Zhang et al., 2010) and do not support the inference of strongly hyperhaline conditions in Lop Nur. Thus, similar to zones 1 and 2, and to a lesser degree to Z3B, carbonate formation in the regions of inflows and dispersal of precipitated carbonate grains in the lake basin are inferred from the $\delta^{18}O_{bulk}$ values of Z4.

The coarser sediments centered at 0.7 and 0.5 m depth were previously described as sand grains that were mostly transported by wind prior to deposition in Lop Nur, and two periods of near-desiccation of Lop Nur were inferred by Mischke et al. (2017). The two sand layers are accompanied by $\delta^{18}O_{bulk}$ maxima with the upper layer corresponding to the highest $\delta^{18}O_{bulk}$ value of the entire section (Fig. 2B,F). Unlike in Z1, sandier sediments are here apparently not reflecting stronger inflows to the lake but result from diminished runoff, stronger evaporative concentration of lake waters, lower lake levels and the enhanced incorporation of mostly aeolian-transported grains in the lake sediments. Mischke et al. (2017) discussed the significance of these sand layers in comparison to other climate records from the region and suggested that water withdrawal for irrigation farming in the upper and middle reaches of Lop Nur's drainage during the westward expansion of the Chinese empire in the Han Dynasty caused an environmental crisis downstream and eventually resulted in the fall of the Loulan Kingdom. The lower abundance of mica in the upper half of Z4 also indicates that the sandier sediments are predominantly aeolian-transported, sedimentologically more mature particles rather than fresh detrital materials delivered by the Tarim and possibly other rivers. The almost complete absence of fossils from Z4 indicates that salinities were probably mostly > 110‰. However, relatively high $\delta^{13}C_{bulk}$ values in Z4 possibly indicate a higher productivity in comparison to Z2 and Z3B. In addition, the presence of ooids during previous periods of relatively low $\delta^{18}O_{bulk}$ values and their occurrence in Z4 suggests salinities below the inferred high levels during the accumulation of the sediments of Z2 and Z3B.

Generally drier climate conditions after the deposition of the Z3 sediments were also inferred by Liu et al. (2016) from relatively high soluble salt contents and predominantly detrital sediments of aeolian origin. Relatively high pollen concentrations, high *Artemisia* and low *Ephedra* counts are in contrast to the inference of arid conditions but high *Pinus* and *Picea* counts indicate a higher portion of far-distance transported pollen and a dry climate (Liu et al., 2016).

SARs were ca. 0.3 mm a^{-1} in Z4. Slightly higher SARs in Z4 in comparison to those in Z3 possibly result from the enhanced contribution of mostly aeolian-transported sands in Z4 (Liu et al., 2016; Mischke et al., 2017). However, generally low SARs in Z4 in comparison to those of Z1 and Z2 are consistent with weak inflows in Lop Nur.

The record from the YKD0301 section implies salinities between ca. 20–100‰ at ca. 9.0 ka (Z1) in Lop Nur. Around 8.8 ka (Z2), salinities were > 110‰. During ca. 8.7–7.5 ka (Z3A), lowest salinities in a range from 0.5–18‰ existed in the lake before high values of > 110‰ (Z3B) were re-established between ca. 7.5–6.0 ka. Another period of low salinity of ca. 5–18‰ (Z3C) prevailed between 6.0 and 5.0 ka. Afterwards, high salinities of > 100‰ existed but probably did not reach the high levels of 8.8 or 7.5–6.0 ka.

4.2. Comparisons with other Holocene records from Lop Nur

A detailed comparison and possibly correlation of the sediments at YKD0301 and other Holocene sediments from the Lop Nur Basin is hampered by the lack of well-dated exposed or drilled sediment sequences. The four drilled cores ZK95–6, K1, L07–10 and Luo 4, and the two excavated pits Ma and F4 yielded Holocene dating results (Fig. 1). Unfortunately, the Holocene units of the individual sediment sequences were not dated by more than three radiocarbon samples. Thus, chronologies are uncertain not only due to the low number of age data but also due to lacking independent age controls required for the assessment of potential lake reservoir effects on radiocarbon dating results. However, the uppermost metres of sediments at the six locations regarded as Holocene deposits are generally fine grained and described as silt and clay or mud (Yan et al., 1983; Zheng et al., 1991; Wang et al., 2000; Liu et al., 2003, 2016; Ma et al., 2008; Hua et al., 2009). Mean grain sizes mostly between 6 and 20 μm at YKD0301 are relatively comparable to generally fine-grained sediments with a reported average median grain size of 8 μm in section Ma and ca. 10 μm in the K1 core (Wang et al., 2000; Ma et al., 2008). The occurrence of gypsum and halite was reported for the Holocene parts of ZK95–6 and the Ma section and significant portions of salt were recorded in core L07–10 and in section YKD0301 (Liu et al., 2003, 2016; Ma et al., 2008; Hua et al., 2009).

Brackish or saline water ostracods such as *C. torosa* and *E. mareotica* were also reported from the Ma and F4 pits and the K1 core (described as the sub-species *C. littoralis* for the latter two locations and as *E. inflata* (a younger synonym) by Zheng et al. (1991), Wang et al. (2000) and Ma et al. (2008)). In addition, the brackish water species *Cyprinotus* sp. (usually identified as *Heterocypris* sp. from the region by western researchers) was recorded at F4 (Zheng et al., 1991). The foraminifer *A. tepida* was recorded in the K1 core in addition to the YKD0301 location (Wang et al. (2000). Both locations lie 22 km apart, and a generally wider distribution of *A. tepida* in early Holocene sediments of Lop Nur is expected. The presence of abundant shells of *C. torosa*, *E. mareotica* and tests of *A. tepida* in sediments relatively reliably dated as early Holocene at the YKD0301 location and their occurrence at the K1 core location, and the reports of the same ostracod species from F4 suggest that abundant remains of the three taxa might be used as stratigraphic marker for early Holocene sediments in the Lop Nur Basin.

Organism remains indicating relatively dilute waters in addition to those recorded in Z3A and Z3C at YKD0301 were only reported from late Holocene sediments of the Ma section (Ma et al., 2008). These sediments even include shells of several gastropods such as *Radix* or *Lymnaea,* and pondweed (*Potamogeton*) fruits. These unique remains in sediments of the Holocene Lop Nur possibly reflect the pit's location close to potential inflow areas of the Tarim and Konqi rivers (Fig. 1).

4.3. Comparison with records from NW China and palaeoclimate implications

Relatively low salinities were reconstructed during the middle Holocene periods between ca. 8.7–7.5 ka and 6.0–5.0 ka in Lop Nur. Pollen data from YKD0301 were very cautiously and only briefly discussed by Liu et al. (2016). However, the largest drop of *Ephedra* pollen in the record at ca. 8.7 ka and highest Gramineae values in the middle Holocene correspond to the inferred periods of lowest salinities in the lake. Thus, dilute lake waters in Lop Nur were probably not or not only triggered by higher temperatures in the region and increased meltwater discharge but resulted from generally wetter climate conditions. Inferred wettest conditions in northwesternmost China and adjacent regions in the earlier half of the Holocene correspond with pollen and other lake records from Lake Karakul, Lake Issyk-Kul, the Yili River Valley and Lake Manas, and with the speleothem records from Kesang Cave (Fig. 1; Sun et al., 1994; Ricketts et al., 2001; Li et al., 2011; Cai et al., 2017; Heinecke et al., 2017).

In contrast, wettest conditions in the second half of the Holocene were inferred for northwesternmost China based on pollen records from Lake Aibi, Lake Balikun, Lake Bosten, Lake Sayram, and Lake Wulungu, on loess-paleosol sequences in the Tian Shan and the Yili River valley and on climate modelling results (Fig. 1; Liu et al., 2008; Huang et al., 2009; An et al., 2011, Jin et al., 2012; Jiang et al., 2013; Wang et al., 2013; Chen et al., 2016).

Discrepancies between individual climate records possibly result

from spatial heterogeneities and are possibly related to catchment-specific characteristics such as the portion of high-alpine regions including water resources stored as ice, snow and frozen ground, and differences in rain-shadow and other local effects. In addition, inferences based on lacustrine pollen records alone are possibly less sound than at least partly regarded due to the high portion of long-distance transported pollen grains and unknown mixtures of pollen grains transported by wind and flowing waters (Zhu et al., 2002; Zhao et al., 2008; Li et al., 2012). Another source of uncertainty is the robustness and precision of mostly radiocarbon- and OSL-dating based chronologies of climate records. It is clear that more detailed analyses are required to assess the wettest Holocene climate conditions in northwesternmost China and adjacent regions in a reliable way.

The salinity record from Lop Nur integrates climate parameters such as precipitation, temperature, evaporation, wind speed and seasonality, and catchment- and basin-specific characteristics such as the contribution of meltwater, and the formation and subsequent dissolution of a salt crust during lake-level falls and rises, respectively. Inferences of controlling climate conditions based on the salinity reconstruction remain speculative. However, the inference of salinities in a range from 20 to 100‰ at ca. 9 ka in Lop Nur which were apparently sufficiently stable to support ostracod and foraminifera populations in the lake is surprising due to reconstructions of dry early Holocene climate conditions from nearby loess-paleosol sequences and records from Lake Bosten and Lake Balikun (Fig. 7; Chen et al., 2016). Both lakes were apparently significantly smaller than today before 9 ka (Wünnemann et al., 2006; An et al., 2011). Earlier reports that the lakes Bosten and Balikun were completely dry before 8 or 9 ka were revised by subsequent studies which indicate the continuous existence of the lakes in the early Holocene (Zhang et al., 2010; An et al., 2011; Zhao et al., 2015; Li et al., 2017). Given that pollen data from Lake Bosten and Lake Balikun indicate dry climate conditions in the early Holocene, a potentially relatively continuous freshwater inflow to Lop Nur which supported the ostracod and foraminifera fauna possibly resulted from strong meltwater discharge to the lake as a result of relatively high temperatures.

Correspondingly, high temperatures at ca. 9 ka were inferred from Lake Wulungu and Lake Sayram (Liu et al., 2008; Jiang et al., 2013). In contrast, pollen data and lake-level reconstructions suggest relatively dry conditions (Fig. 7). However, glacier ice, accumulated in the high mountain ranges surrounding the Tarim Basin during the SWHTS 2A in the Younger Dryas period apparently provided a sufficient meltwater inflow in Lop Nur during the early Holocene to maintain salinities of 20–100‰ in the lake although precipitation did possibly not yet reach Holocene peak values (Huang et al., 2009; Dortch et al., 2013). Similar arguments were used to explain low $\delta^{18}O$ values in the stable isotope record from Lake Issyk-Kul before 8.3 ka (Ricketts et al., 2001). The meltwater discharge to Lop Nur was probably more significant from the high mountain ranges along the Tarim Basin, i.e., the southern-central Tian Shan and the Kunlun Shan which feed the Tarim and the Cherchen rivers. In contrast, meltwater discharge was probably significantly lower from the eastern-central Tien Shan drained by the Kaidu River due to the inference of a low level of Lake Bosten before 8.2 ka (Wünnemann et al., 2006).

5. Conclusions

The fossil and stable isotope data from the YKD0301 section show that Lop Nur experienced large salinity variations in the Holocene. Apart from two periods of more dilute waters in the middle Holocene, salinities were mostly hyperhaline in the lake. The onset of most dilute conditions in the lake at ca. 8.7 ka coincides with transitions from a dry climate to significantly wetter conditions at Lake Bosten and Lake Balikun (Fig. 7; Wünnemann et al., 2006; Huang et al., 2009; An et al.,

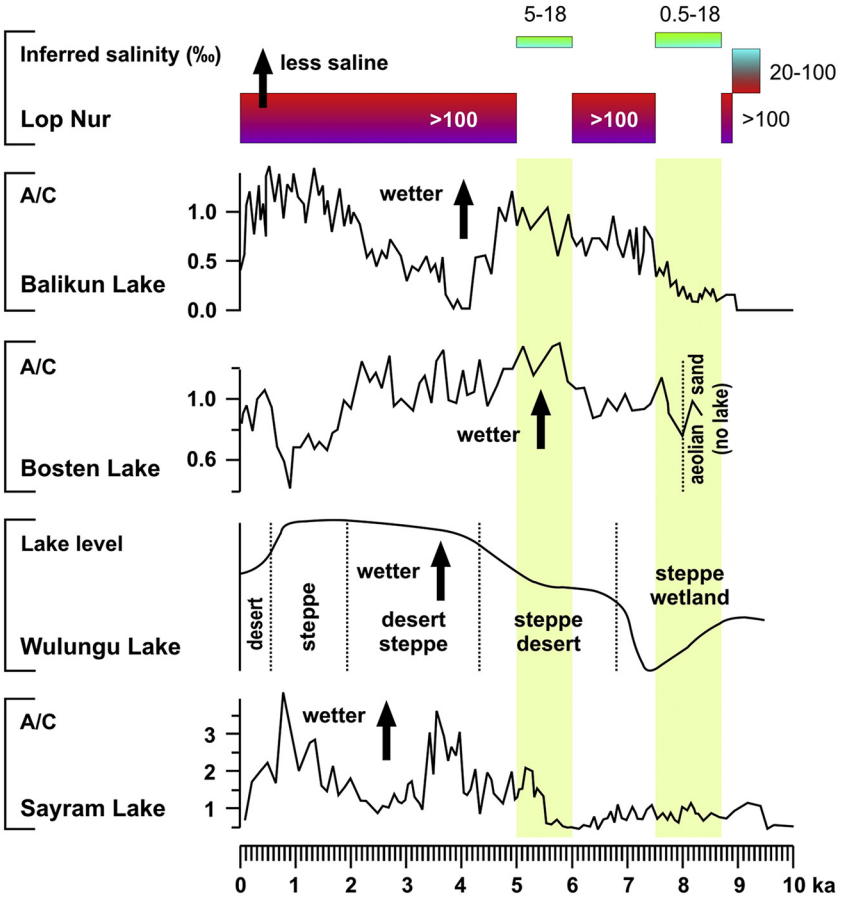

Fig. 7. Comparison of the salinity record from Lop Nur (this study) with climate records from the lakes Sayram, Wulungu, Bosten and Balikun (Liu et al., 2008; Huang et al., 2009; Tao et al., 2010; Jiang et al., 2013). Green vertical bars indicate the two periods of most dilute waters in Lop Nur. A/C is the *Artemisia*/Chenopodiaceae ratio. (For interpretation of the references to colour in this figure legend, the reader is referred to the web version of this article.)

2011). However, the period of the reconstructed lowest salinity in Lop Nur between 8.7 and 7.5 ka significantly precedes periods of wettest climate conditions inferred from these two lakes (Fig. 7). Inconsistencies among these and other lake records from the region possibly result from catchment-specific differences in meltwater contribution, different controls on salinity (precipitation, temperature, evaporation, wind speed, ice cover, presence of salt crusts, etc.) in comparison to more typical palaeoclimate proxies such as pollen, and dating uncertainties.

Abundant shells of *C. torosa* and *E. mareotica*, and tests of *A. tepida* only in the lowermost sediments of the YKD0301 section suggest that this assemblage might be used as stratigraphic indicator of early Holocene sediments in the Lop Nur Basin.

The distribution of ooids in sediments of Lop Nur is here reported for the first time. Their formation in Lop Nur is another example for the possibility that ooids in ancient hard rocks were formed in a saline-lake environment and not necessarily in a marine setting. The ooids from Lop Nur should be investigated in more detail to assess their potential as stratigraphic markers, and to better understand their specific conditions of formation.

Supplementary data to this article can be found online at https://doi.org/10.1016/j.gloplacha.2019.01.017.

Acknowledgements

We are indebted to Ahuva Almogi-Labin (Geological Survey of Israel) for help with *Ammonia tepida* identification and ecological assessment, to Sveinbjörn Steinþórsson (University of Iceland) for thin section preparation and Philipp Hoelzmann (Free University of Berlin, Germany) for XRD analysis of ooids. The comments and suggestions of two reviewers helped to improve the original manuscript version. Funding was provided by China's NSF projects (40830420, 41771004) and the National 305 Project of the Ministry of Science and Technology of China (2003BA612A-06-15).

References

Almogi-Labin, A., Perelis-Grossovicz, L., Raab, M., 1992. Living *Ammonia* from a hypersaline inland pool, Dead Sea area. Israel. J. Foramin. Res. 22, 257–266.
An, C.-B., Lu, Y., Zhao, J., Tao, S., Dong, W., Li, H., Jin, M., Wang, Z., 2011. A high-resolution record of Holocene environmental and climatic changes from Lake Balikun (Xinjiang, China): implications for central Asia. The Holocene 22, 43–52.
Ban, G., 1962. 92. Han Dynasty. Reprinted by Zhonghua Book Company, Beijing (1962).
Bathurst, R.G.C., 1971. Carbonate Sediments and their Diagenesis. Elsevier, New York, pp. 620.
Cai, Y., Chiang, J.C.H., Breitenbach, S.F.M., Tan, L., Cheng, H., Edwards, R.L., An, Z., 2017. Holocene moisture changes in western China, Central Asia, inferred from stalagmites. Quat. Sci. Rev. 158, 15–28.
Chen, F., Jia, J., Chen, J., Li, G., Zhang, G., Zhang, X., Xie, H., Xia, D., Huang, W., An, C., 2016. A persistent Holocene wetting trend in arid central Asia, with wettest conditions in the late Holocene, revealed by multi-proxy analyses of loess-paleosol sequences in Xinjiang, China. Quat. Sci. Rev. 146, 134–146.
Dai, L., Gong, Y., Li, X., Feng, W., Yu, Y., 2014. Influence of environmental factors on zooplankton assemblages in Bosten Lake, a large oligosaline lake in arid northwestern China. Sci. Asia 40, 1–10.
Davaud, E., Girardclos, S., 2001. Recent freshwater ooids and oncoids from western Lake Geneva (Switzerland): indications of a common organically mediated origin. J. Sediment. Res. 71, 423–429.
Davis, J.S., Lipkin, Y., 1986. *Lamprothamnium* prosperity in permanently hypersaline water. Schweiz. Z. Hydrol. 48, 240–246.
Dong, Z., Lv, P., Qian, G., Xia, X., Zhao, Y., Mu, G., 2012. Research progress in China's Lop Nur. Earth-Sci. Rev. 111, 142–153.
Dortch, J.M., Owen, L.A., Caffee, M.W., 2013. Timing and climatic drivers for glaciation across semi-arid western Himalayan-Tibetan orogeny. Quat. Sci. Rev. 78, 188–208.
Drapun, I., Anufriieva, E., Shadrin, N., Zagorodnyaya, Y., 2017. Ostracods in the plankton of the Sivash Bay (the Sea of Azov) during its transformation from brackish to hypersaline state. Ecologica Montenegrina 14, 102–108.
Halley, R.B., 1977. Ooid fabric and fracture in the Great Salt Lake and the geologic record. J. Sediment. Petrol. 47, 1099–1120.
Hao, H., Ferguson, D.K., Chang, H., Li, C.-S., 2012. Vegetation and climate of the Lop Nur area, China, during the past 7 million years. Clim. Change 113, 323–338.
Hedin, S., 1942. Der wandernde See. Brockhaus, Leipzig (295 pp).
Heinecke, L., Mischke, S., Adler, K., Barth, A., Biskaborn, B.K., Plessen, B., Nitze, I., Kuhn, G., Rajabov, I., Kuhn, G., Herzschuh, U., 2017. Climatic and limnological changes at Lake Karakul (Tajikistan) during the last 29 cal ka BP. J. Paleolimnol. 58, 317–334.
Hem, J.D., 1982. Conductance: A Collective Measure of Dissolved Ions. In: Minear, R.A., Keith, L.H. (Eds.), Water Analysis, Inorganic Species, Part 1. Vol. 1. Academic Press, New York, pp. 137–161.
Hofmann, J., Mischke, S., Schudack, M., 2002. Formation, age and ostracod ecology of palaeo-lake deposits in the Gangou valley, eastern Tian Shan (NW-China). Zeitschrift für Geomorphologie N.F., Suppl.-Bd. 126, 115–129.
Horton, T.W., Defliese, W.F., Tripati, A.K., Oze, C., 2016. Evaporation induced ^{18}O and ^{13}C enrichment in lake systems: a global perspective on hydrologic balance effects. Quat. Sci. Rev. 131, 365–379.
Hou, X., 2001. Vegetation Atlas of China. Science Press, Beijing, pp. 260 (in Chin.).
Hua, Y.S., Jiang, P.A., Wu, H.Q., Zhong, J.P., Ma, L.C., Li, B.G., 2009. The sedimentary characteristics of Profile L07-10 and its environmental indicator in Lop Nor Great Ear area. J. Xinjiang Agricult. Univ. 32, 36–39 (in Chin. with Engl. abstract).
Huang, X.Z., Chen, F.H., Fan, Y.X., Yang, M.L., 2009. Dry late-glacial and early Holocene climate in arid central Asia indicated by lithological and palynological evidence from Bosten Lake, China. Quat. Int. 194, 19–27.
Jiang, Q., Ji, J., Shen, J., Matsumoto, R., Tong, G., Qian, P., Ren, X., Yan, D., 2013. Holocene vegetational and climatic variation in westerly-dominated areas of Central Asia inferred from the Sayram Lake in northern Xinjiang, China. Sci. China Earth Sci. 56, 339–353.
Jin, L., Chen, F., Morrill, C., Otto-Bliesner, B.L., Rosenbloom, N., 2012. Causes of early Holocene desertification in arid central. Asia. Clim. Dynamics 38, 1577–1591.
Kantrud, H.A., 1991. Wigeongrass (*Ruppia maritima* L.): a literature review. U.S. Fish and Wildlife Service, Fish and Wildlife Research 10, 58.
Keatings, K.W., Hawkes, I., Holmes, J.A., Flower, R.J., Leng, M.J., Abu-Zied, R.H., Lord, A.R., 2007. Evaluation of ostracod-based palaeoenvironmental reconstruction with instrumental data from the arid Faiyum Depression, Egypt. J. Paleolimnol. 38, 261–283.
Kelts, K., Sharabi, M., 1986. Holocene sedimentology of hypersaline Lake Urmia, northwestern Iran. Palaeogeogr. Palaeoclimatol. Palaeoecol. 54, 105–130.
Li, X., Liu, W., 2010. Oxygen isotope fractionation in the ostracod *Eucypris mareotica*: results from a culture experiment and implications for paleoclimate reconstruction. J. Paleolimnol. 43, 111–120.
Li, B., Ma, L., Jiang, P., Duan, Z., Sun, D., Qiu, H., Zhong, J., Wu, H., 2008. High precision topographic data on Lop Nor basin's Lake “Great Ear”? and the timing of its becoming a dry salt lake. Chin. Sci. Bull. 53, 905–914.
Li, X., Zhao, K., Dodson, J., Zhou, X., 2011. Moisture dynamics in central Asia for the last 15 kyr: new evidence from Yili Valley, Xinjiang, NW China. Quat. Sci. Rev. 30, 3457–3466.
Li, Y., Wang, N., Li, Z., Zhang, C., Zhou, X., 2012. Reworking effects in the Holocene Zhuye Lake sediments: A case study by pollen concentrates AMS ^{14}C dating. Sci. China Earth Sci. 55, 1669–1678.
Li, G., Rao, Z., Duan, Y., Xia, D., Wang, L., Madsen, D.B., Jia, J., Wei, H., Qiang, M., Chen, J., Chen, F., 2016. Paleoenvironmental changes recorded in a luminescence dated loess/paleosol sequence from the Tianshan Mountains, arid central Asia, since the penultimate glaciation. Earth Planet. Sci. Lett. 448, 1–12.
Li, G., Duan, Y., Huang, X., Buylaert, J.-P., Peng, W., Madsen, D.B., Rao, Z., She, L., Xie, H., Chen, J., Chen, F., 2017. The luminescence dating chronology of a deep core from Bosten Lake (NW China) in arid central Asia reveals lake evolution over the last 220 ka. Boreas 46, 264–281.
Liu, C.L., Wang, M.L., Jiao, P.C., Li, S., Chen, Y.Z., 2003. Holocene yellow silt layers and the paleoclimate event of 8200 a BP in Lop Nur, Xinjiang, NW China. Acta Geol. Sin. (Engl. Ed.) 77, 514–518.
Liu, X., Herzschuh, U., Shen, J., Jiang, Q., Xiao, X., 2008. Holocene environmental and climatic changes inferred from Wulungu Lake in northern Xinjiang, China. Quat. Res. 70, 412–425.
Liu, C., Zhang, J., Jiao, P., Mischke, S., 2016. The Holocene history of Lop Nur and its palaeoclimate implications. Quat. Sci. Rev. 148, 163–175.
Ma, C., Wang, F., Cao, X., Li, S., Li, X., 2008. Climate and environment reconstruction during the Medieval Warm Period in Lop Nur of Xinjiang, China. Chin. Sci. Bull. 53, 3016–3027.
Ma, L., Lowenstein, T.K., Li, B., Jiang, P., Liu, C., Zhong, J., Sheng, J., Qiu, H., Wu, H., 2010. Hydrochemical characteristics and brine evolution paths of Lop Nor Basin, Xinjiang Province, Western China. Appl. Geochem. 25, 1770–1782.
Meisch, C., 2000. Freshwater Ostracoda of Western and Central Europe. Spektrum, Heidelberg (522 pp).
Mischke, S., Schudack, M.E., 2001. Sub-Recent Ostracoda from Bosten Lake, NW China. J. Micropalaeontol. 20, 12.
Mischke, S., Zhang, C., 2011. Ostracod distribution in Ulungur Lake (Xinjiang, China) and a reassessed Holocene record. Ecol. Res. 26, 133–145.
Mischke, S., Hofmann, J., Schudack, M.E., 2004. Ostracod ecology of alluvial loess deposits in an eastern Tian Shan palaeo-lake (NW China). In: Smykatz-Kloss, W., Felix-Henningsen, P. (Eds.), Palaeoecology of Quaternary Drylands. Lecture Notes in Earth Sciences. Vol. 102. Springer, Berlin, pp. 219–231.
Mischke, S., Herzschuh, U., Massmann, G., Zhang, C., 2007. An ostracod-conductivity transfer-function for Tibetan lakes. J. Paleolimnol. 38, 509–524.
Mischke, S., Kramer, M., Zhang, C., Shang, H., Herzschuh, U., Erzinger, J., 2008. Reduced early Holocene moisture availability in the Bayan Har Mountains, northeastern Tibetan Plateau, inferred from a multi-proxy lake record. Palaeogeogr. Palaeoclimatol. Palaeoecol. 267, 59–76.
Mischke, S., Liu, C., Zhang, J., Zhang, C., Zhang, H., Jiao, P., Plessen, B., 2017. The world's earliest Aral-Sea type disaster: the decline of the Loulan Kingdom in the Tarim Basin. Sci. Rep. 7, 43102.
Prejevalsky, N.M., 1879. From Kulja, across the Tian Shan to Lob-Nor. Translated by E.D. Morgan. Including Notices of the Lakes of Central Asia. Sampson Low, Marston.

Searle & Rivington, London, pp. 251.
Ran, M., Zhang, C., Feng, Z., 2015. Climatic and hydrological variations during the past 8000 years in northern Xinjiang of China and the associated mechanisms. Quat. Int. 358, 21–34.
Ricketts, R.D., Johnson, T.C., Brown, E.T., Rasmussen, K.A., Romanovsky, V.V., 2001. The Holocene paleolimnology of Lake Issyk-Kul, Kyrgyzstan: trace element and stable isotope composition of ostracodes. Palaeogeogr. Palaeoclimatol. Palaeoecol. 176, 207–227.
Sandberg, P.A., 1975. New interpretations of Great Salt Lake ooids and ancient non-skeletal carbonate mineralogy. Sedimentology 22, 427–537.
Schornikov, E.I., 1964. An experiment on the distinction of the Caspian elements of the ostracod fauna in the Azov-Black Sea Basin. Zoologicheski Zhurnal 43, 1276–1293.
Shadrin, N., Anufriieva, E., 2012. Review of the biogeography of *Artemia* Leach, 1819 (Crustacea: Anostraca) in Russia. Int. J. *Artemia* Biol. 2, 51–61.
Simone, L., 1981. Ooids: a review. Earth-Sci. Rev. 16, 319–355.
Sun, X.J., Du, N.Q., Wong, C.Y., Lin, R.F., Wei, K.Q., 1994. Paleovegetation and paleoenvironment of Manas Lake, Xinjiang, N.W. China during the last 14,000 years. Quat. Sci. 3, 239–246 (in Chin. with Engl. abstract).
Sun, X., Liu, C., Jiao, P., Yan, H., Chen, Y., Ma, L., Zhang, Y., Wang, C., Li, W., 2016. A further discussion on genesis of potassium-rich brine in Lop Nur: Evaporating experiments for brine in gypsum-bearing clastic strata. Mineral Deposits 35, 1190–1204 (in Chin. with Engl. abstract).
Tao, S.C., An, C.B., Chen, F.H., Tang, L.Y., Wang, Z.L., Lü, Y.B., Li, Z.F., Zheng, T.M., Zhao, J.J., 2010. Pollen-inferred vegetation and environmental changes since 16.7 ka BP at Balikun Lake, Xinjiang. Chin. Sci. Bull. 55, 2449–2457.
Vanhaecke, P., Tackaert, W., Sorgeloos, P., 1987. The biogeography of *Artemia*: an updated review. In: Sorgeloos, P., Bengtson, D.A., Decleir, W., Jaspers, E. (Eds.), Artemia Research and its Applications. Ecology, Culturing, Use in Aquaculture. Universa Press, Wetteren, pp. 129–155.
Vanhaeke, P., Siddall, S.E., Sorgeloos, P., 1984. International study on *Artemia*. XXXII. Combined effects of temperature and salinity on the survival of *Artemia* of various geographical origin. J. Exp. Mar. Biol. Ecol. 80, 259–275.
von Grafenstein, U., Erlenkeuser, H., Trimborn, P., 1999. Oxygen and carbon isotopes in modern fresh-water ostracod valves: assessing vital offsets and autoecological effects of interest for palaeoclimate studies. Palaeogeogr. Palaeoclimatol. Palaeoecol. 148, 133–152.
Walton, R., Sloan, B.J., 1990. The genus *Ammonia* Bruennich, 1772: its geographic distribution and morphologic variability. J. Foramin. Res. 20, 128–156.
Wang, M., Huang, X., Liu, C., Li, H., Zhao, Z., 1999. The discovery of foraminiferal fossils in cores from hole KI in Lop Nur. Xinjiang. Geol. Rev. 45, 158–162 (in Chin. with Engl. abstract).
Wang, M., Pu, Q., Liu, C., Chen, Y., 2000. Quaternary climate and environment in the Lop Nur, Xinjiang. Acta Geol. Sin. 74, 273–278.
Wang, W., Feng, Z., Ran, M., Zhang, C., 2013. Holocene climate and vegetation changes inferred from pollen records of Lake Aibi, northern Xinjiang, China: a potential contribution to understanding of Holocene climate pattern in East-central Asia. Quat. Int. 311, 54–62.
Warren, J.K., 2006. Evaporites: Sediments, Resources and Hydrocarbons. Springer, Berlin, pp. 1036.
Wilkinson, B.H., Pope, B.N., Owen, R.M., 1980. Nearshore ooid formation in a modern temperate region marl lake. J. Geol. 88, 697–704.
Williams, W.D., 1991. Chinese and Mongolian saline lakes: a limnological overview. Hydrobiologia 210, 39–66.
Wünnemann, B., Mischke, S., Chen, F., 2006. A Holocene sedimentary record from Bosten lake, China. Palaeogeogr. Palaeoclimatol. Palaeoecol. 234, 223–238.
Yan, F., Ye, Y., Mai, X., 1983. The sporo-pollen assemblage in the Luo-4 drilling of Lop Lake in Uygur Autonomous Region of Xinjiang and its significance. Seismol. Geol. 5, 75–80 (in Chin. with Engl. abstract).
Yang, X., Liu, Z., Zhang, F., White, P.D., Wang, X., 2006. Hydrological changes and land degradation in the southern and eastern Tarim Basin, Xinjiang, China. Land Degrad. Dev. 17, 381–392.
Zhang, C., Feng, Z., Yang, Q., Gou, X., Sun, F., 2010. Holocene environmental variations recorded by organic-related and carbonate-related proxies of the lacustrine sediments from Bosten Lake, northwestern China. The Holocene 20, 363–373.
Zhang, J.F., Liu, C.L., Wu, X.H., Liu, K.X., Zhou, L.P., 2012. Optically stimulated luminescence and radiocarbon dating of sediments from Lop Nur (Lop Nor), China. Quat. Geochron. 10, 150–155.
Zhao, Y., Yu, Z., Chen, F., Li, J., 2008. Holocene vegetation and climate change from a lake sediment record in the Tengger Sandy Desert, northwest China. J. Arid Environ. 72, 2054–2064.
Zhao, Y., An, C., Mao, L., Zhao, J., Tang, L., Zhou, A., Li, H., Dong, W., Duan, F., Chen, F., 2015. Vegetation and climate history in arid western China during MIS2: New insights from pollen and grain-size data of the Balikun Lake, eastern Tien Shan. Quat. Sci. Rev. 126, 112–125.
Zheng, M., Qi, W., Wu, Y., 1991. Sedimentary environment since the Late Pleistocene and prospect of potash development in the Lop Nur salt lake. Chin. Sci. Bull. 36, 1810–1813 (in Chin.).
Zhu, Y., Chen, F., Cheng, B., Zhang, J., Madsen, D.B., 2002. Pollen assemblage features of modern water samples from the Shiyang River drainage, arid region of China. Acta Bot. Sin. 44, 367–372.